Insect hapto-electrical stimulation of Venus flytrap triggers exocytosis in gland cells

Authors: Sönke Scherzer[1], Lana Shabala[2], Benjamin Hedrich[2†], Jörg Fromm[3], Hubert Bauer[1], Eberhard Munz[4], Peter Jakob[5], Khaled Al-Rascheid[6], Ines Kreuzer[1], Dirk Becker[1], Monika Eiblmeier[7], Heinz Rennenberg[7], Sergey Shabala[2], Malcolm Bennett[8], Erwin Neher[9*] and Rainer Hedrich[1*]

Affiliations:

[1] Institute for Molecular Plant Physiology and Biophysics, University Wuerzburg, D-97070 Wuerzburg, Germany;

[2] School of Land and Food, University of Tasmania, Hobart, TAS, Australia;

[3] Universität Hamburg, Zentrum Holzwirtschaft, D-21031 Hamburg, Germany;

[4] Leibniz Institute of Plant Genetics and Crop Plant Research, D- 06466 Gatersleben, Germany

[5] Experimental Physics 5, University of Würzburg, D-97070 Wuerzburg, Germany;

[6] Zoology Department, College of Science, King Saud University, Riyadh 11451, Saudi Arabia;

[7] Chair of Tree Physiology, Institute of Forest Sciences, University of Freiburg, D-79110 Freiburg, Germany;

[8] Centre for Plant Integrative Biology, School of Biosciences, University of Nottingham, LE12 5RD, UK;

[9] Department for Membrane Biophysics, Max Planck Institute for Biophysical Chemistry, D-37077 Goettingen, Germany

*Correspondence to: R.H. (hedrich@botanik.uni-wuerzburg.de) or E.N. (eneher@gwdg.de).

[†]Present address: Medical University of Graz, 8010 Graz, Austria

Abstract

The Venus flytrap *Dionaea muscipula* captures insects and consumes their flesh (1, 2). Prey contacting touch-sensitive hairs trigger travelling electrical waves. These action potentials (APs) cause rapid closure of the trap and activate secretory functions of glands, which cover its inner surface (3, 4). Such prey-induced hapto-electric stimulation activates the touch hormone jasmonate (JA) signaling pathway, which initiates secretion of an acidic hydrolase cocktail to decompose the victim and acquire the animal nutrients (5-7). Although postulated since Darwin's pioneering studies these secretory events have not been recorded so far. Using advanced analytical and imaging techniques, such as vibrating ion selective electrodes, carbon fiber amperometry and MRI, we monitored stimulus-coupled glandular secretion into the flytrap. Trigger hair bending or direct application of JA caused a quantal release of oxidizable material from gland cells monitored as distinct amperometric spikes. Spikes reminiscent of exocytotic events in secretory animal cells progressively increased in frequency, reaching steady state one day after stimulation. Our data indicate that trigger hair mechanical stimulation evokes APs. Gland cells translate APs into touch-inducible JA signalling that promotes the formation of secretory vesicles. Early vesicles loaded with H^+ and Cl^- fuse with the plasma membrane, hyper-acidifying the 'green stomach´-like digestive organ, while subsequent ones carry hydrolases and nutrient transporters together with a glutathione redox moiety, which is likely to act as the major detected compound in amperometry. Hence, when glands perceive the hapto-electrical stimulation, secretory vesicles are tailored to be released in a sequence, which optimizes digestion of the captured animal.

Significance statement:

The Venus flytrap has been in the focus of scientists since Darwin's time. Carnivorous plants, with their specialized lifestyle, including insect capture, as well as digestion and absorption of

prey, developed unique tools to gain scarce nutrients. In this study we describe novel mechanistic insights into the cascade of events following the capture of insect prey. Action potentials evoked by the struggling prey are translated into touch-inducible hormone signals that promote the formation of secretory vesicles. A variety of digestive compounds are released sequentially into the flytrap's 'green stomach' and break down the captured animal. Amperometry provides insight into the kinetics and chemistry of the stimulus-coupled glandular secretion process**.**

\body

Introduction:

Certain plants have turned the sword; they capture and consume animals, including potential herbivores. Growing on mineral-deficient soils, the carnivorous Venus flytrap (*Dionaea muscipula*) lures (8), captures, and digests small arthropods, in order to feed on the nutrients extracted from their flesh (1, 3, 9-12). Closure of the bilobed snap trap is initiated by mechanical stimulation of trigger hairs located at the inner trap surface. Each trigger hair bending elicits the firing of an action potential (AP). With the first AP, the trap stays open, but memorizes the initial strike. If a second one fires within 20 s, it triggers rapid trap closure. In case an insect is trapped and struggles to escape, two and more hapto-electric stimuli activate jasmonate signaling and biosynthesis (3, 6, 7). From the fifth strike on, glands raise their expression levels of hydrolase and nutrient transporter genes. When mechano-stimulation is replaced by application of coronatine (COR), a mimic of the biologically active jasmonate hormone JA-Ile, it can substitute for the mechano-electric stimulation of the flytrap (7). Hapto-electric signaling and touch hormone activation turn the closed trap into a 'green stomach', flooding the entrapped prey with an acidic digestive fluid (3, 6, 13). Although prey capture and consumption of the Venus flytrap has been known since Darwin's time (2), the molecular mechanisms of fluid phase secretion underlying animal consumption remained unknown (14). In this study

amperometric carbon fibers were used for the first time in the plant field to monitor the dynamics and kinetics of mechano-electric and JA stimulation of the secretory events, providing insight into exocytosis-dependent liquor filling of the digestive organ.

Results:

Upon hapto-electric trap activation the surface area of the multicellular gland cell complex increases by 30% and an acidic protein moiety is released into the 'green stomach' formed by the hermetically sealed lobes of the trap (3, 5-7, 13). In search of the membrane reservoir responsible for the surface increase of stimulated glands, we exposed traps to the JA-Ile mimic coronatine (COR). 48 h after stimulus onset membrane pits, observed in electron micrographs (EM) of glands suggested that secretory vesicle fusion had taken place predominantly at the apical end of head cells (outermost cell layer; L1) (Fig. 1 and S3B). Head cells of non-stimulated glands only occasionally showed exocytotic vesicles (1.5 ± 0.4 per cell; Fig. 1A and C) but in the outermost layer of jasmonate-stimulated glands cells, we detected a pronounced increase of pits associated with the more apical plasma membrane sections (16.5 ± 1.5 per cell, approximately 0.18 µm in diameter; Fig. 1B, D and E). These results indicate that the secretory stimulation causes granule docking and membrane fusion.

<u>MIFE resolves early secretion of acidic vesicles</u>

In a previous study, we compared the transcriptomic profile of non-stimulated glands with that of glands stimulated either by insects or COR. Before stimulation, the transcription profile of resting glands is already dominated by secretory processes (7). *Dionaea* secretion is directly coupled to acidification; H^+ and chloride, Cl^-, are released into the digestive fluid of the tightly sealed trap (15). To test whether touch stimulation of the flytrap's trigger hairs is translated into ion fluxes across the gland plasma membrane, we used Ca^{2+}, Cl^-, and H^+ sensitive MIFE microelectrodes (3, 16), which measure fluxes by recording local concentration gradients. After

5 - 10 consecutive trigger-hair stimulations and a lag time of about 10 min, a rapid shift in the net ion fluxes towards net Ca^{2+} uptake into the gland cells was observed (Fig. 2A). The mean net Ca^{2+} flux after mechanical stimulation (5 APs) of the Venus flytrap was about 9.9 ± 1.8 nmol m^{-2} s^{-1} (Fig. 2B; mean ± SE, n = 6). Within the first hour following stimulation, the ion fluxes were dominated by Ca^{2+} fluxes. Upon Ca^{2+} entry, the intracellular Ca^{2+} level rises (6), and JA signaling is activated (3, 7). Either consecutive trigger hair stimulation alone or a direct application of jasmonates or COR induces secretion. With jasmonates secretion in traps is initiated before they close (6). Following application of JAs, however, Ca^{2+} sensitive MIFE electrodes did not record net Ca^{2+} flux into glands (Fig. 2A, B; red symbols/bar). Hormone stimulation however, triggered proton release, which appeared within 5 - 10 min following stimulation onset (Fig. 2C, D). Net H^+ efflux reached its peak between 1 and 2.5 h after stimulus application and then gradually recovered (Fig. 2C). When comparing the time that glands required to reach peak proton extrusion in response to mechanical or chemical stimulation, JAs were the fastest (Fig. 2C). Thus jasmonate-induced proton release was significantly faster than that elicited by mechanical stimulation (insert in Fig. 2C), which reached peak currents of 54 ± 7 nmol m^{-2} s^{-1} (mean ± SE, n = 6). Also the lag time of H^+ efflux resulting from the different stimulations was longest in response to mechanical stimulation (Fig. 2D). This time dependence fits the notion that the rise in gland JA is downstream of hapto-electrics and gland calcium entry.

Regardless of whether stimulated or not, the resting membrane potential of glands remained in the range of -120 to -140 mV (12). This might indicate that trap acidification results from electroneutral exocytotic H^+ release rather than the massive activation of plasma membrane proton pumps. This notion is supported by the COR induced increase in vacuolar AHA10-type proton pump transcripts (17), together with those of a ClC-type proton-chloride antiporter (18), two components required for hyper-acidification of secretory vesicles (see Fig. S1 and supplementary text S1). To test whether H^+ fluxes are accompanied by Cl^- fluxes, we used

chloride-sensitive MIFE electrodes side-by-side with the pH microelectrodes. Confirming our working model, we monitored pronounced Cl^- net efflux from glands in COR stimulated (Fig. 2E; blue symbols), but not in resting (Fig 2E; grey symbols) traps. COR induced chloride currents appeared with a similar time dependence and amplitude as the proton fluxes (Fig. 2C, E). Both fluxes were correlated with each other ($R^2 = 0.61$; $P < 0.01$), exhibiting a stoichiometry between H^+ and Cl^- close to 1:1 (Fig. 2F). The electrochemistry-based MIFE experiments illustrated above can only be conducted in an aqueous environment. In such a wet scenario, we monitored initial secretion-associated proton extrusion in response to COR about 9 min after stimulation (Fig. 2D). To resolve the onset of gross gland fluid secretion in the initially dry *Dionaea* trap, we followed the fluid production after COR stimulation by Infra Red Gas Analysis (IRGA) and magnetic resonance imaging (MRI). First fluid phase secretion-associated trap water vapor emission was detected in IRGA recordings 151 ± 13 min (n = 3, mean ± SD) following trap stimulation with COR (Fig. S2A). After reaching peak humidity trap water emission slowly decreased and suddenly dropped after 445 ± 84 min (n = 3, mean ± SD) to the basal level of evaporation prior to COR application and non-stimulated controls (Fig. S2A). This rapid drop in water emission reflects hermetical sealing of the trap lobes (6). Filling of the closed trap with digestive fluid was visualized by MRI imaging (Fig. S2B and supplementary video 1).

Detection of digestive vesicles via Amperometry

With animal cells exocytotic events can be monitored non-invasively via amperometry, detecting redox currents when electrodes are placed near the membrane surface of secretory cells (19, 20). Given that amperometry detects oxidizable substances such as neurotransmitters, neuropeptides and hormones released from secretory vesicles, we adopted this electrochemical approach to probe for exocytotic events in active flytrap glands. Aiming to detect spikes associated with secretory cargo release from inner trap surface, we placed carbon fiber

microelectrodes in contact with the apical face of the glands upper head cells (Fig. S3A and B). Under these experimental conditions no amperometric signals were detectable in non-stimulated glands (Fig. S3C). However, with glands stimulated by 5 - 20 trigger hair displacements, signals similar to those measured with secretory animal cells could be monitored (21, 22) (Fig. 3A), albeit with a much slower time course due to cell wall geometry. When placing two electrodes next to each other both electrodes recorded characteristic increases in amperometric current in close temporal relationship, as shown in Fig. 3A and B, excluding the possibility, that such discrete events were artifacts generated in one or the other electrode. In these experiments we had to use strong pH-buffering in order to preserve the sensitivity of the amperometric electrodes (see Methods).

The amperometrically detected chemical species is released to the apoplast at the point of exocytosis. From that point source the released substance diffuses to the electroactive tip of the carbon fiber where it is oxidized. It has been shown that placing electrodes more than several microns away from the cell surface results in a significant decrease in signal and spatio-temporal resolution (23, 24). Therefore, the best scenario for detecting exocytotic events without diffusional dilution is to actually touch the cell surface with the electrode. This limitation by diffusion can be described by Fick's law. Thus we fitted the amperometrically detected spikes with a 3D diffusion equation according to eq. 1 (see Methods). From this calculation we gained a parameter t_c, which is a characteristic diffusion time, depending on the distance between the point source of secretion and the carbon fiber tip, given a certain diffusion coefficient D. Fitting sharp secretory events observed when electrodes were placed directly on the *Dionaea* gland surface with a high spatio-temporal resolution, resulted in t_c-values of about 4-5 s. Plotting the relative signal abundance against the calculated t_c-values of detected secretory events, a broadly homogenous distribution was obtained (Fig. S3D). In other words, the amperometric approach we used, detects secretory events originating from various distances to the tip of the carbon fiber, or else implies a range of diffusion coefficients. Interestingly, we

did not obtain any t_c-values ≤ 3.25 s in 63 analyzed spikes. Assuming a constant D-value in the performed experiments and $t_c \geq 3.25$ s, we can calculate a lower bound for the geometrical distance between the point of secretion and the carbon fiber (eq.2, see methods) and D (diffusion constant of the secreted substance in the medium) ((2) see Methods). In contrast to animal cells, the plasma membrane of plant cells is covered with an extra layer of cellulose-based cell wall and a lipid-based cuticle. Thus the minimal t_c-value obtained for *Dionaea* glands very likely results from the cell wall-cuticle shell that keeps the fiber electrode at some distance (r) from exocytotic vesicles fusing with the gland cell plasma membrane. From electron micrographs similar to those shown in figure 1 we calculated a minimal distance between electrode and secreted vesicle fusing with the head gland cell plasma membrane of ~0.5 µm (Fig. 1B). Introducing this value in the equation (2) we are able to calculate the diffusion constant (D) of the *Dionaea* secreted fluid in its diffusion medium (containing the cell wall and cuticle). The calculated value of $D = 1.92 \times 10^{-10}$ cm²/s indicates a high diffusional resistance of the gland cell wall. For comparison, the diffusion coefficient of dopamine in water was reported with 6.0×10^{-6} cm²/s (25). Also in the animal system diffusion in tissue or in solutions containing biological macromolecules is known to be hindered by the cellular matrix. Hafez et al. (26) have reported that the diffusion coefficient of dopamine at the surface of an adrenal cell is one-tenth compared to its diffusion in water. The small diffusion constant reported here for *Dionaea* also illustrates the slow time characteristics of the detected amperometrical spikes with a half-life ($t_{1/2}$) time constant of 87.82 ± 12.14 s (mean ± SE; n = 92). Compared to the free aqueous diffusion of catecholamine release in neuronal cells, $t_{1/2}$ of *Dionaea* plant secretory events is enlarged by a factor of ~10,000 (24, 26).

To determine emergence and manifestation of gland cell exocytosis, we monitored the frequency of secretory events for up to 145 h. Traps were stimulated either mechanically by a series of 20 consecutive trigger hair bendings or by spraying COR onto the traps´ inner surface. Within the first 4 - 5 h after stimulation onset, no significant signals could be monitored. First

exocytosis-type spiking was observed after about 6 h (Fig. 3D). Thereafter, exocytotic events occurred more frequently, reaching about half-maximum spiking after 12 - 13 h. Maximal spiking rates were detected after 24 h and remained high for another 2 days before slowly declining at days 4 and 6 (Fig. 3D). Interestingly, COR stimulation and trigger hair bendings resulted in a similar time dependence of spiking frequency. This indicates that jasmonate induction of secretory vesicle formation, loading and membrane fusion, rather than touch induction of jasmonate biosynthesis, represents the rate-limiting step during *Dionaea* gland cell exocytosis.

We also found that the Ca^{2+} channel blocker gadolinium strongly reduced the volume of secreted fluid (supplementary video 2). In order to further investigate the inhibitory effect of Gd^{3+} on trap secretory fluid production, traps were sprayed with 10 mM Gd^{3+} (~2.5 µmol) 24 h before mechanical stimulation. This Gd^{3+} challenge did, however, not affect the traps´ naturally fast closure in response to two trigger hair strikes. When traps were mechanically stimulated for secretion by 5 - 20 trigger hair displacements, gadolinium sprayed traps were found to be strongly reduced in extruded fluid volume. Compared to control traps, which secreted 2.12 ± 0.67 µl/1000 glands within 48 h, Gd^{3+} pretreated traps released only 0.35 ± 0.25 µl/1000) (Fig. 3C, black bars). At the same time, exocytotic events amperometrically determined with single gland cells dropped from 14.3 ± 4.17 events/h in controls to 2.1 ± 2.45 events/h in the Gd^{3+} exposed traps (Fig. 3C, red bars). The pronounced Gd^{3+} block of secretion seen by amperometry and MRI suggests that JA and calcium signaling is required for hapto-electric and JA stimulation of *Dionaea* gland cell secretion.

What kind of redox moiety *Dionaea's* secretory gland cells release? In order to gain and maintain functional integrity of cysteine-rich hydrolytic enzymes exuded into the digestive fluid (13, 27, 28), a defined redox status in the extracellular bioreactor is required. Glutathione (GSH) represents an important redox regulator of enzyme functions in plant cells (29, 30). Glutathione is synthesized via a well-known enzymatic pathway (see Fig. S4). Glutathione can be derived

from activated sulfate (APS, adenosine 5´- phosphosulfate) via a well-known enzymatic pathway (see Fig. S4). Gene expression analysis based on RNAseq data (available at http://tbro.carnivorom.com, c.f. (7)) indicated that coronatine might induce genes involved in GSH production and transport. These analyses were further confirmed by quantitative RT-PCR. Among these genes the APS reductase (DmAPR3) is strongly upregulated 12 h after COR stimulation (Fig. 4B). APS reductase represents the most important regulatory enzyme of the pathway that determines the flux of sulfate into organic sulfur compounds in plants (31) (for review see (32)). In addition, the availability of C-N skeletons for cysteine synthesis is promoted in response to the JA mimic through enhanced serine O-acetyltransferase (DmSERAT2) expression, and cysteine synthesis by itself, via elevated O-acetylserine(thiol)lyase (DmOASTL) expression (Fig. 4C, (33)). Moreover, the putative GSH transporter DmOPT6 is transcriptionally induced after COR treatment as well. Interestingly, all four transcripts are induced by both COR or prey capture in a similar fashion (Fig. 4B-D and http://tbro.carnivorom.com). Therefore, enhanced sulfate reduction and assimilation seems to be required for both the synthesis of cysteine rich hydrolytic enzymes and additional synthesis of glutathione, which can be detected in the secreted fluid.

To test whether glutathione is released into the extracellular compartment, we sampled digestive fluids from stimulated flytraps and analyzed the samples for the presence of anti-oxidants (34-36). Indeed, we could detect GSH in *Dionaea´s* extracellular fluid (Fig. 4A). In contrast to glutathione however, ascorbate was not detectable by state-of-the-art methods (36, 37). While the GSH concentration in whole *Dionaea* traps was not significantly altered by COR treatment, the stomach glutathione concentration was in the order of 10 µM 48 h after stimulation onset (Fig. 4A, red bars). In order to test the sensitivity of the used carbon fibers in our amperometric analysis towards this ROS scavenger, we performed experiments with defined GSH concentrations (Fig. S3E). In these experiments the reduced GSH was oxidized at

the positively charged carbon fiber resulting in a positive current. Interestingly, the amperometric current detected with a constant potential of +900 mV in solutions of defined GSH concentrations saturated with a half maximal concentration (K_m) of 10 µM (Fig. S3E), which corresponds well with the actual GSH concentration in the secreted fluid. Thus it is likely that under our conditions secreted GSH is detected in the amperometric analysis. Nevertheless, we expect the amperometry to detect also additional electroactive substances besides GSH released in the secreted fluid of stimulated Venus flytraps.

Discussion:

The molecular machinery underlying secretory vesicle fusion with the plasma membrane in animal cells is known in great detail (38-40). Upon chemical or electrical stimulation of secretory animal cells, exocytotic events can be detected within milliseconds (41-44). In these fast responding cells, certain pools of preformed cargo-loaded vesicles are released immediately after stimulus onset. Following hapto-electric calcium entry in *Dionaea* glands jasmonate-signalling triggers vesicle acidification and *de novo* synthesis of secretory proteins. The fact that carbon fiber electrodes detect amperometric signals not earlier than about 6 h after mechanical- and JA stimulation (Fig. 3D) may indicate that the oxidizable compound, most likely the tripeptide glutathione, is contained only in those vesicles equipped with hydrolases. In the acidic extracellular digestive fluid glutathione is very stable, providing for a proper redox state for sustained hydrolase activity (45).

Dionaea's secretion events occur on a slow timescale. The apparent diffusion constant of released substances, as calculated from the waveform of the amperometric signal, was D = 1.92×10^{-10} cm²/s, which indicates a high diffusional resistance of the gland cell wall. For comparison, the diffusion constant of catecholamines in aqueous solution is 1×10^{-6} to 8×10^{-7} cm²/s (19, 46). Thus diffusion in the cell wall of *Dionaea* glands is about four orders of

magnitude slower than that of small molecules in aequeous solution. In contrast to fast synaptic signaling in the nervous system of animals, this slow diffusion as well as the slow time course of release reflects the biology of the insect-processing flytrap: Once *Dionaea* captures prey via its fast hapto-electric sensing system, exocytotic release and slow diffusion of a tailored hydrolase cocktail into the digestive fluid perfectly serves the long-term nutrient needs of the plant.

Material and Methods:

Amperometric Recordings

In order to access the inner trap surface even in stimulated plants, unstimulated traps in the open position were fixed in a chamber and mechanically locked to prevent trap closure upon stimulation. For inhibitor pre-treatments, plants were sprayed with 10 mM $GdCl_3$, or H_2O as control. 24 h after pre-treatments traps were stimulated for secretion either mechanically (touch of trigger hairs, 5 - 10 times within 1 min) or by hormone spraying (100 µM COR). At the given time points after stimulation amperometric measurements were performed with open fixed traps still attached to the plant. The chamber was filled with standard bath solution (1 mM KCl, 1 mM $CaCl_2$, 50 mM HEPES/NaOH pH 7) and placed on a microscope stage (Zeiss Axioscope 2 FS, Germany). A three-electrode configuration was employed where an Ag/AgCl electrode served as the reference electrode grounding the bath solution. Two sensory carbon fiber electrodes of 5 µm diameter (ALA Scientific Instruments, Westbury, NY) were used for amperometric detection. Carbon fibers were gently placed on top of the gland head cells if not stated otherwise. During amperometric recordings, electrodes were held at +900 mV with two VA-10X amperometry amplifiers (ALA Scientific Instruments). Oxidative current was acquired via VA-10X and digitized at 20 kHz through an ITC-18 digital to analog convertor (InstruTECH, NY). Data were acquired using Patch master (HEKA Elektronik, Germany) and

analyzed with a custom-written fit running under Igor 6. Detected events were described by following equations (47):

$$f(x) = M / (t-t_0)^{1.5} * \exp(-t_c / (t-t_0)) \quad (1)$$

Here, t_0 is the time of signal onset (a free fitting parameter), and M depends on the amount of secreted substance as well as on the diffusion coefficient D. The parameter t_c depends on D and the distance, r, between the point source of secretion and the carbon fiber tip according to:

$$t_c = r^2 / 4\,D \quad (2)$$

Further details on Materials and Methods can be found in 'Supplementary Materials and Methods'.

Author Contributions:

E.N., and R.H. conceived the work; S.S. conducted initial feasibility studies; S.S., I.K., L.Sh., S.Sh., H.R., D.B., E.N., P.J., K.A.S. A.-R., and R.H. designed the experiments and analysed the data; S.S., I.K., L.Sh., J.F., H.B., M.E., E.M., and B.H. performed the experiments; and S.S., I.K., D.B., E.N., M.B., and R.H. wrote the manuscript.

Acknowledgments: We thank B. Neumann and P. Winter for technical assistance. This work was supported by the German Plant Phenotyping Network (DPPN) and by the European Research Council under the European Union's Seventh Framework Programme (FP/20010-2015) / ERC Grant Agreement n. [250194-Carnivorom]. This work was also supported by the International Research Group Program (IRG14-08), Deanship of Scientific Research, King Saud University, Saudi Arabia (to H.R., N.E., and A.R.K.)

The authors declare no competing financial interests

References:

1. Ellison AM & Gotelli NJ (2009) Energetics and the evolution of carnivorous plants--Darwin's 'most wonderful plants in the world'. *J. Exp. Bot.* 60(1):19-42.
2. Darwin C (1875) *Insectivorous Plants* (Murray, London, UK).
3. Böhm J, *et al.* (2016) The Venus Flytrap *Dionaea muscipula* Counts Prey-Induced Action Potentials to Induce Sodium Uptake. *Curr. Biol.* 26(3):286-295.
4. Robins RJ & Juniper BE (1980) The Secretory Cycle of *Dionaea-Muscipula Ellis* .3. The Mechanism of Release of Digestive Secretion. *New Phytol.* 86(3):313-327.
5. Libiakova M, Flokova K, Novak O, Slovakova L, & Pavlovic A (2014) Abundance of cysteine endopeptidase dionain in digestive fluid of Venus flytrap (*Dionaea muscipula Ellis*) is regulated by different stimuli from prey through jasmonates. *PLoS One* 9(8):e104424.
6. Escalante-Perez M, *et al.* (2011) A special pair of phytohormones controls excitability, slow closure, and external stomach formation in the Venus flytrap. *Proc. Natl. Acad. Sci. U. S. A.* 108(37):15492-15497.
7. Bemm F, *et al.* (2016) Venus flytrap carnivorous lifestyle builds on herbivore defense strategies. *Genome Res.* 26(6):812-825.
8. Kreuzwieser J, *et al.* (2014) The Venus flytrap attracts insects by the release of volatile organic compounds. *J. Exp. Bot.* 65(2):755-766.
9. Adamec L (1997) Mineral nutrition of carnivorous plants: A review. *Bot. Rev.* 63(3):273-299.
10. Böhm J, *et al.* (2016) Venus Flytrap HKT1-Type Channel Provides for Prey Sodium Uptake into Carnivorous Plant Without Conflicting with Electrical Excitability. *Mol Plant* 9(3):428-436.
11. Scherzer S, *et al.* (2015) Calcium sensor kinase activates potassium uptake systems in gland cells of Venus flytraps. *Proc. Natl. Acad. Sci. U. S. A.* 112(23):7309-7314.
12. Scherzer S, *et al.* (2013) The *Dionaea muscipula* ammonium channel DmAMT1 provides NH_4^+ uptake associated with Venus flytrap's prey digestion. *Curr. Biol.* 23(17):1649-1657.
13. Schulze WX, *et al.* (2012) The protein composition of the digestive fluid from the venus flytrap sheds light on prey digestion mechanisms. *Mol. Cell. Proteomics* 11(11):1306-1319.
14. Robins RJ & Juniper BE (1980) The Secretory Cycle of *Dionaea-Muscipula Ellis* .1. The Fine-Structure and the Effect of Stimulation on the Fine-Structure of the Digestive Gland-Cells. *New Phytol.* 86(3):279-&.
15. Rea PA, Joel DM, & Juniper BE (1983) Secretion and Redistribution of Chloride in the Digestive Glands of *Dionaea-Muscipula Ellis* (Venus Flytrap) Upon Secretion Stimulation. *New Phytol.* 94(3):359-366.
16. Shabala L, Ross T, McMeekin T, & Shabala S (2006) Non-invasive microelectrode ion flux measurements to study adaptive responses of microorganisms to the environment. *FEMS Microbiol. Rev.* 30(3):472-486.
17. Aprile A, *et al.* (2011) Expression of the H^+-ATPase AHA10 proton pump is associated with citric acid accumulation in lemon juice sac cells. *Funct. Integr. Genomics* 11(4):551-563.
18. Ahnert-Hilger G & Jahn R (2011) CLC-3 spices up GABAergic synaptic vesicles. *Nat. Neurosci.* 14(4):405-407.
19. Wightman RM, *et al.* (1991) Temporally resolved catecholamine spikes correspond to single vesicle release from individual chromaffin cells. *Proc. Natl. Acad. Sci. U. S. A.* 88(23):10754-10758.
20. Chow RH, von Rüden L, & Neher E (1992) Delay in Vesicle Fusion Revealed by Electrochemical Monitoring of Single Secretory Events in Adrenal Chromaffin Cells. *Nature* 356(6364):60-63.
21. Chow RH, Klingauf J, Heinemann C, Zucker RS, & Neher E (1996) Mechanisms Determining the Time Course of Secretion in Neuroendocrine Cells. *Neuron* 16(2):369-376.
22. Mosharov EV (2008) Analysis of single-vesicle exocytotic events recorded by amperometry. *Methods Mol. Biol.* 440:315-327.
23. Jankowski JA, Schroeder TJ, Ciolkowski EL, & Wightman RM (1993) Temporal Characteristics of Quantal Secretion of Catecholamines from Adrenal-Medullary Cells. *J. Biol. Chem.* 268(20):14694-14700.
24. Wightman RM, Schroeder TJ, Finnegan JM, Ciolkowski EL, & Pihel K (1995) Time-Course of Release of Catecholamines from Individual Vesicles during Exocytosis at Adrenal-Medullary Cells. *Biophys. J.* 68(1):383-390.
25. Gerhardt G & Adams RN (1982) Determination of Diffusion-Coefficients by Flow-Injection Analysis. *Anal. Chem.* 54(14):2618-2620.
26. Hafez I, *et al.* (2005) Electrochemical imaging of fusion pore openings by electrochemical detector arrays. *Proc. Natl. Acad. Sci. U. S. A.* 102(39):13879-13884.
27. Paszota P, *et al.* (2014) Secreted major Venus flytrap chitinase enables digestion of Arthropod prey. *Biochim. Biophys. Acta* 1844(2):374-383.

28. Takahashi K, *et al.* (2011) A cysteine endopeptidase ("dionain") is involved in the digestive fluid of *Dionaea muscipula* (Venus's fly-trap). *Biosci. Biotechnol. Biochem.* 75(2):346-348.
29. Scheibe R & Dietz KJ (2012) Reduction-oxidation network for flexible adjustment of cellular metabolism in photoautotrophic cells. *Plant Cell Environ.* 35(2):202-216.
30. Noctor G, *et al.* (2012) Glutathione in plants: an integrated overview. *Plant Cell Environ.* 35(2):454-484.
31. Scheerer U, *et al.* (2010) Sulphur flux through the sulphate assimilation pathway is differently controlled by adenosine 5'-phosphosulphate reductase under stress and in transgenic poplar plants overexpressing gamma-ECS, SO, or APR. *J. Exp. Bot.* 61(2):609-622.
32. Rennenberg H & Herschbach C (2014) A detailed view on sulphur metabolism at the cellular and whole-plant level illustrates challenges in metabolite flux analyses. *J. Exp. Bot.* 65(20):5711-5724.
33. Takahashi H, Kopriva S, Giordano M, Saito K, & Hell R (2011) Sulfur Assimilation in Photosynthetic Organisms: Molecular Functions and Regulations of Transporters and Assimilatory Enzymes. *Annu. Rev. Plant Biol.* 62(1):157-184.
34. Schupp R & Rennenberg H (1988) Diurnal Changes in the Glutathione Content of Spruce Needles (Picea-Abies L). *Plant Science* 57(2):113-117.
35. Strohm M, *et al.* (1995) Regulation of Glutathione Synthesis in Leaves of Transgenic Poplar (Populus-Tremula X Populus-Alba) Overexpressing Glutathione Synthetase. *Plant J.* 7(1):141-145.
36. Arab L, *et al.* (2016) Acclimation to heat and drought-Lessons to learn from the date palm (Phoenix dactylifera). *Environ. Exp. Bot.* 125:20-30.
37. Herschbach C, Scheerer U, & Rennenberg H (2010) Redox states of glutathione and ascorbate in root tips of poplar (*Populus tremulaxP-alba*) depend on phloem transport from the shoot to the roots. *J. Exp. Bot.* 61(4):1065-1074.
38. Leszczyszyn DJ, *et al.* (1991) Secretion of catecholamines from individual adrenal medullary chromaffin cells. *J. Neurochem.* 56(6):1855-1863.
39. Chow RH, Klingauf J, & Neher E (1994) Time course of Ca^{2+} concentration triggering exocytosis in neuroendocrine cells. *Proc. Natl. Acad. Sci. U. S. A.* 91(26):12765-12769.
40. Vukasinovic N & Zarsky V (2016) Tethering Complexes in the *Arabidopsis* Endomembrane System. *Front Cell Dev Biol* 4:46.
41. Tse A & Lee AK (2000) Voltage-gated Ca^{2+} channels and intracellular Ca^{2+} release regulate exocytosis in identified rat corticotrophs. *J Physiol* 528 Pt 1:79-90.
42. Klingauf J & Neher E (1997) Modeling buffered Ca^{2+} diffusion near the membrane: implications for secretion in neuroendocrine cells. *Biophys. J.* 72(2 Pt 1):674-690.
43. Rizzoli SO & Betz WJ (2005) Synaptic vesicle pools. *Nat. Rev. Neurosci.* 6(1):57-69.
44. Koh DS & Hille B (1997) Modulation by neurotransmitters of catecholamine secretion from sympathetic ganglion neurons detected by amperometry. *Proc. Natl. Acad. Sci. U. S. A.* 94(4):1506-1511.
45. Jocelyn PC (1972) Biochemistry of the SH group; the occurrence, chemical properties, metabolism and biological function of thiols and disulphides. (London, New York, Academic Press).
46. Rice ME, Gerhardt GA, Hierl PM, Nagy G, & Adams RN (1985) Diffusion coefficients of neurotransmitters and their metabolites in brain extracellular fluid space. *Neuroscience* 15(3):891-902.
47. Jackson MB (2006) Molecular and Cellular Biophysics (Cambridge University Press, Cambridge).
48. Shi CY, *et al.* (2015) Citrus PH5-like H(+)-ATPase genes: identification and transcript analysis to investigate their possible relationship with citrate accumulation in fruits. *Frontiers in plant science* 6:135.
49. Picollo A & Pusch M (2005) Chloride/proton antiporter activity of mammalian CLC proteins ClC-4 and ClC-5. *Nature* 436(7049):420-423.
50. Robertson JL, Kolmakova-Partensky L, & Miller C (2010) Design, function and structure of a monomeric ClC transporter. *Nature* 468(7325):844-847.
51. Scheel O, Zdebik AA, Lourdel S, & Jentsch TJ (2005) Voltage-dependent electrogenic chloride/proton exchange by endosomal CLC proteins. *Nature* 436(7049):424-427.
52. Spurr HW, Holcomb GE, Hildebrandt AC, & Riker AJ (1964) Distinguishing Tissue of Normal + Pathological Origin on Complex Media. *Phytopathology* 54(3):339-&.
53. Reynolds ES (1963) Use of Lead Citrate at High Ph as an Electron-Opaque Stain in Electron Microscopy. *J. Cell Biol.* 17(1):208-&.
54. Shabala L, Ross T, McMeekin T, & Shabala S (2006) Non-invasive microelectrode ion flux measurements to study adaptive responses of microorganisms to the environment. *FEMS Microbiol. Rev.* 30(3):472-486.
55. Shabala SN, Newman IA, & Morris J (1997) Oscillations in H^+ and Ca^{2+} Ion Fluxes around the Elongation Region of Corn Roots and Effects of External pH. *Plant Physiol* 113(1):111-118.

56. Samuilov S, Lang F, Djukic M, Djunisijevic-Bojovic D, & Rennenberg H (2016) Lead uptake increases drought tolerance of wild type and transgenic poplar (*Populus tremula x P. alba*) overexpressing gsh 1. *Environ. Pollut.* 216:773-785.
57. Duyn JH, Yang Y, Frank JA, & van der Veen JW (1998) Simple correction method for k-space trajectory deviations in MRI. *J Magn Reson* 132(1):150-153.

Figures:

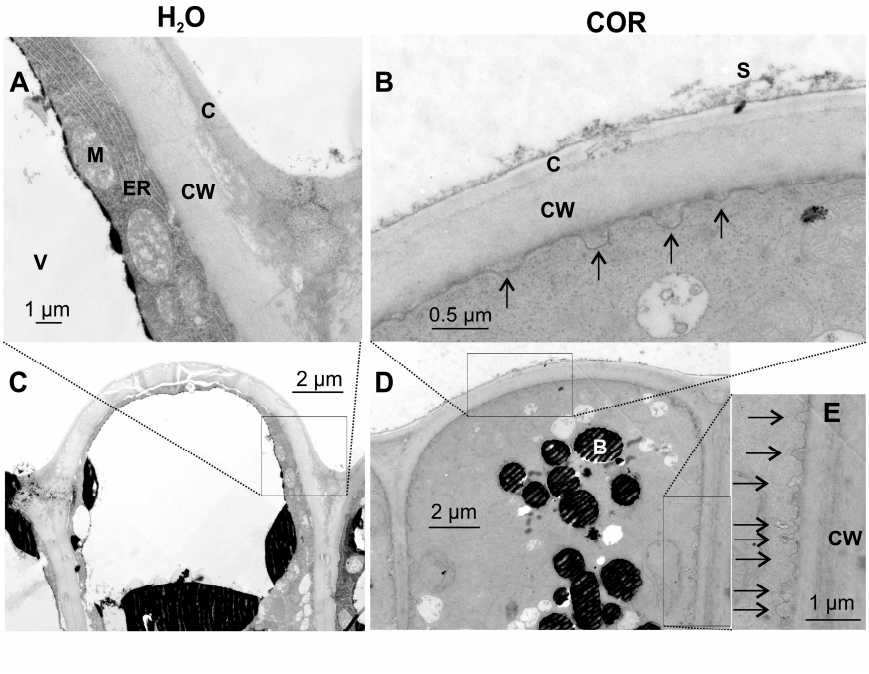

Fig. 1 Exocytotic vesicle fusion is stimulated in activated gland complexes.

Electron micrographs of the outer layer of resting (**A** and **C**) and COR-stimulated (**B**, **D** and **E**) *Dionaea* gland complexes. **A**, **B** and **E** detailed view, **C** and **D** overview. Whereas resting glands do only exhibit few exocytotic events, a massive rise in exocytotic vesicle fusion with the plasma membrane (black arrows) could be detected 48 h after COR stimulation. B, dark stained body; C, cuticle; CW, cell wall; ER, endoplasmic reticulum; M, mitochondria; S, secreted fluid; V, vacuole.

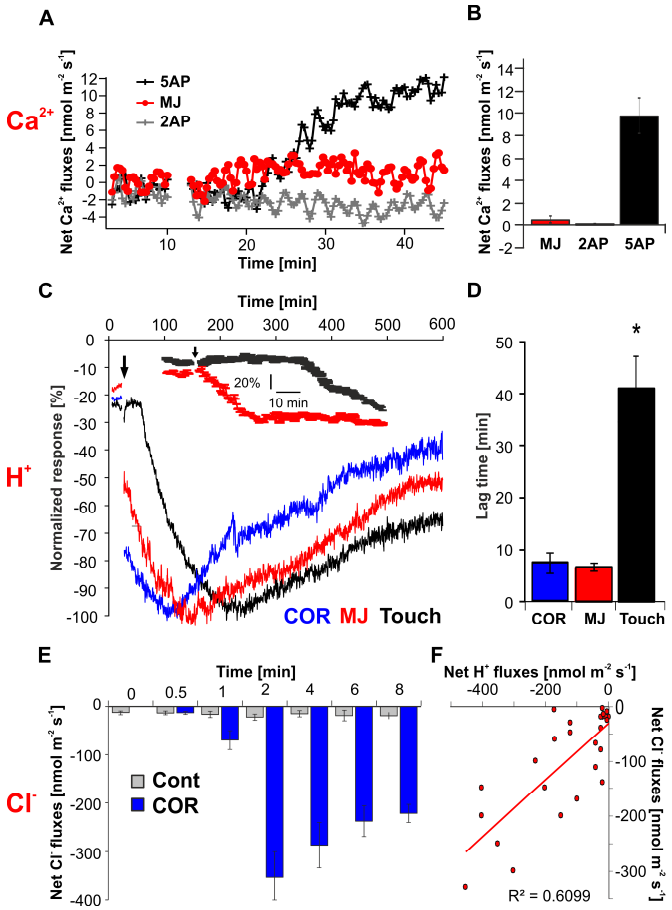

Fig 2 Net ion fluxes measured from stimulated *Dionaea* glands via MIFE technique.

A) Net Ca^{2+} flux in response to mechanical (touched for either 2 or 5 times within 10 sec) and chemical stimulation (1 mM methyl jasmonate, MJ). **B)** Peak Ca^{2+} flux response values for data shown in panel A (mean ± SE; n ≥ 5). **C)** H^+ flux kinetics in response to touch and Jasmonate stimulation. Each flux was normalized to its maximum flux (100%) to illustrate the difference in the peak time (mean ± SE; n ≥ 5). Insert: comparison of touch and MJ treatments at high temporal resolution. **D)** Lag time in H^+ flux responses between treatments shown in panel C. Jasmonate-induced proton release was significantly faster compared to mechanical induction ($p \leq 0.01$; one way Anova). **E)** Net Cl^- fluxes measured in COR stimulated (blue bars) and non-stimulated (grey bars) glands at various time points after stimulation (mean ± SE; n ≥ 4). **F)** Correlation of net H^+ and Cl^- fluxes measured from COR stimulated glands at different time points illustrated in panel **E**. Each point represents a separate measurement. For all MIFE flux data, the sign convention is 'influx positive'.

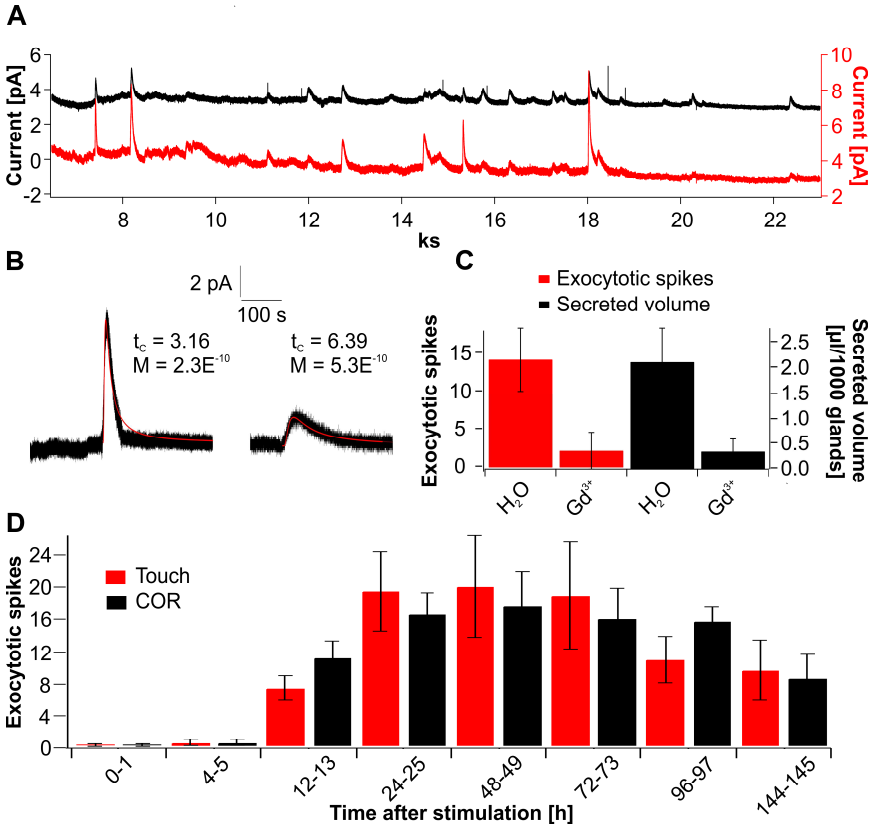

Fig 3 Amperometric detection of exocytotic events in *Dionaea glands*

A) Long-term spiking response of stimulated glands. Current spikes resulting from the exocytosis of individual vesicles were detected with 2 electrodes simultaneously clamped to +900 mV. **B)** Two examples of analyzed exocytotic current spikes are shown. Fitting these events with equation (1) $f(x) = M / (t-t_0)^{1.5} * \exp(-t_c / (t-t_0))$ (red line) reveals characteristics of release quantified by M and t_c which reflect amount and distance of fusing vesicle to carbon fiber. **C)** 10 mM Gadolinium was sprayed 24 h before mechanical stimulation of the Venus flytraps. 24 h after stimulation the number of amperometrical detected events within 1 h (red) and the secreted volume (black) was calculated. Compared to control traps, gadolinium inhibits secretion as well as amperometrically detectable exocytotic spiking. Data are mean ± SD ($n \geq 25$). **D)** Time course of exocytosis related spiking in response to touch (red) and COR (black). For the given time points number of exocytotic events were calculated. Both stimuli lead to the same long-term spiking response in flytrap glands. Data represent mean ± SD ($n \geq 54$).

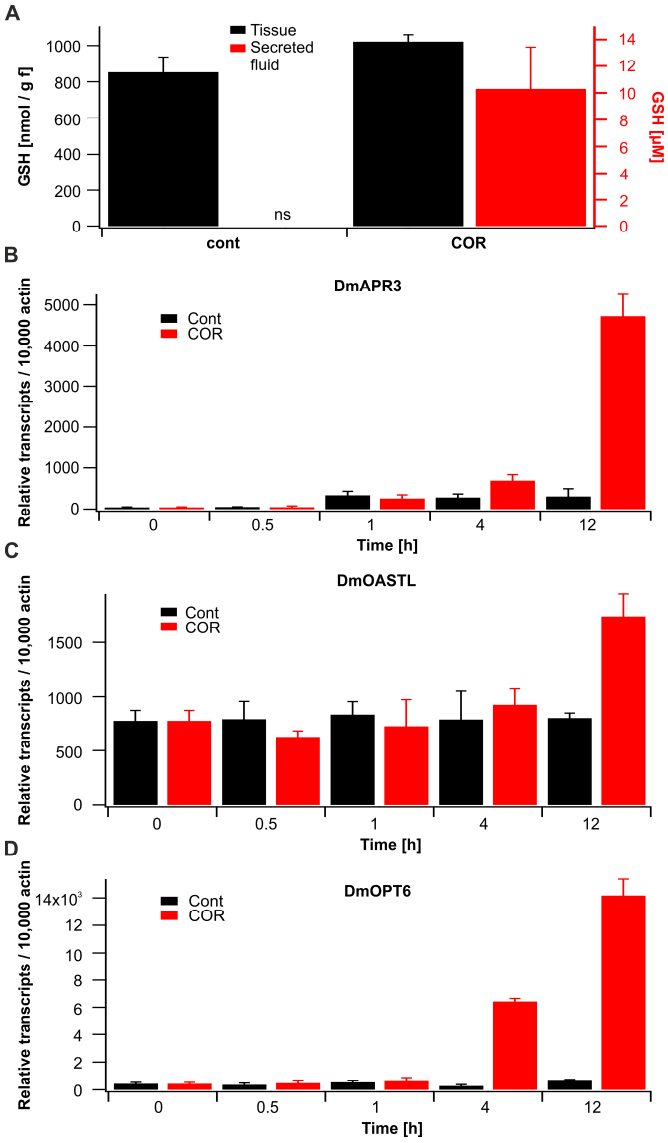

493

494 **Fig 4 Synthesis of the ROS scavenger Glutathione is induced in stimulated *Dionaea* traps**

495 **A)** GSH levels in traps (black) or secreted fluid (red bars) under non-stimulated conditions

496 (control) or 24 h after spray application of 100 µM COR. Please note that resting traps do not

497 secrete (ns) digestive fluid. Data represent mean ± SD (n ≥ 4). **B)-D)** Coronatine induces key

498 genes involved in GSH biosynthesis. Expression of DmAPR3, DmOASTL and DmOPT6 in

499 *Dionaea* gland complexes. Traps were sprayed with water (control, black) or 100 µM COR

500 (red) and gland complexes harvested at the time points indicated. Transcript numbers are given

501 relative to 10,000 molecules of DmACT1; (mean ± SE, n = 6).